Per. Mineral. (2001), *70*, 1, 71-97 http://go.to/permin

PERIODICO di MINERALOGIA
established in 1930

An International Journal of
MINERALOGY, CRYSTALLOGRAPHY, GEOCHEMISTRY,
ORE DEPOSITS, PETROLOGY, VOLCANOLOGY
and applied topics on *Environment, Archaeometry* and *Cultural Heritage*

Quantitative distribution and chemical composition of authigenic minerals in clinoptilolite-bearing ignimbrites from northern Sardinia (Italy): inferences for minerogenetic models

PAOLA MORBIDELLI[1], MARIA ROSARIA GHIARA[2]*, ROBERTO LONIS[3] and CARMELA PETTI[4]

[1] Via Bacchilide 12, I-00125 Roma, Italy
[2] Dipartimento di Scienze della Terra, Università «Federico II», Via Mezzocannone 8, I-80134 Napoli, Italy
[3] Progemisa, S.p.A., Via Contivecchi 7, I-09122 Cagliari, Italy
[4] Centro Musei delle Scienze Naturali, Università «Federico II», Via Mezzocannone 8, I-80134 Napoli, Italy

Submitted, December 2000 - Accepted, March 2001

ABSTRACT. — This paper describes the quantitative distribution and chemical compositions of the main authigenic phases occurring in Tertiary zeolite-bearing ignimbrites from northern Sardinia. Previous studies had indicated clinoptilolite as the most widespread authigenic mineral, with minor amounts of smectite, mordenite and silica minerals. Quantitative analyses using the combined Rietveld-RIR (Reference Intensity Ratio) method showed that, on a regional scale, clinoptilolite amounts ranging from 20 wt% to 30 wt% may be considered realistic; however, several levels of ignimbrites and related deposits revealed relative abundances for large-scale mining (>50 wt%).

The chemical composition of the clinoptilolites, ranging from K to Ca varieties, and distribution within the volcanic piles strongly support changes in the compositions of the interacting fluids.

The overall quantitative and chemical data confirm and define better the previous minerogenetic models carried out for the poorly welded ignimbritic deposits, which are mainly based on alteration processes of glassy components dominated by entrapped cognate fluids. On the other hand, external fluids are required for epiclastic and *base surges* deposits.

* Corresponding author, E-mail: mghiara@unina.it

RIASSUNTO. — In questo lavoro vengono riportate le variazioni composizionali, quantitative e distributive delle zeoliti e delle principali fasi secondarie ad esse associate nei flussi piroclastici pomiceo cineritici Terziari della Sardegna settentrionale e nei depositi epiclastici e di *base surges* ad essi correlati. Un precedente studio aveva messo in evidenza che la clinoptilolite, associata a subordinate mordenite, smectite e minerali della silice, è la zeolite maggiormente diffusa.

Le analisi quantitative, effettuate con il metodo combinato Rietveld-RIR, indicano che, su scala regionale, un contenuto medio in clinoptilolite variabile fra il 20 e 30% in peso può essere considerato realistico. Tuttavia, alcuni livelli ignimbritici, epiclastici e dei *base surges*, raggiungono concentrazioni di rilevante interesse economico (>50% in peso).

Le clinoptiloliti variano da termini potassici a termini calcici e suggeriscono, durante i processi di alterazione della componente vetrosa delle ignimbriti, cambiamenti della composizione chimica dei fluidi interagenti.

Sia i dati quantitativi che quelli chimici confermano e meglio definiscono i modelli minerogenetici precedentemente proposti per le zeoliti e per le fasi ad esse associate nei flussi cineritici poco saldati; l'insieme dei dati suggerisce che un ruolo primario, nel processo di alterazione, è svolto dai fluidi presenti nei flussi ignimbritici. Per i depositi epiclastici ed quelli di tipo *base surge*,

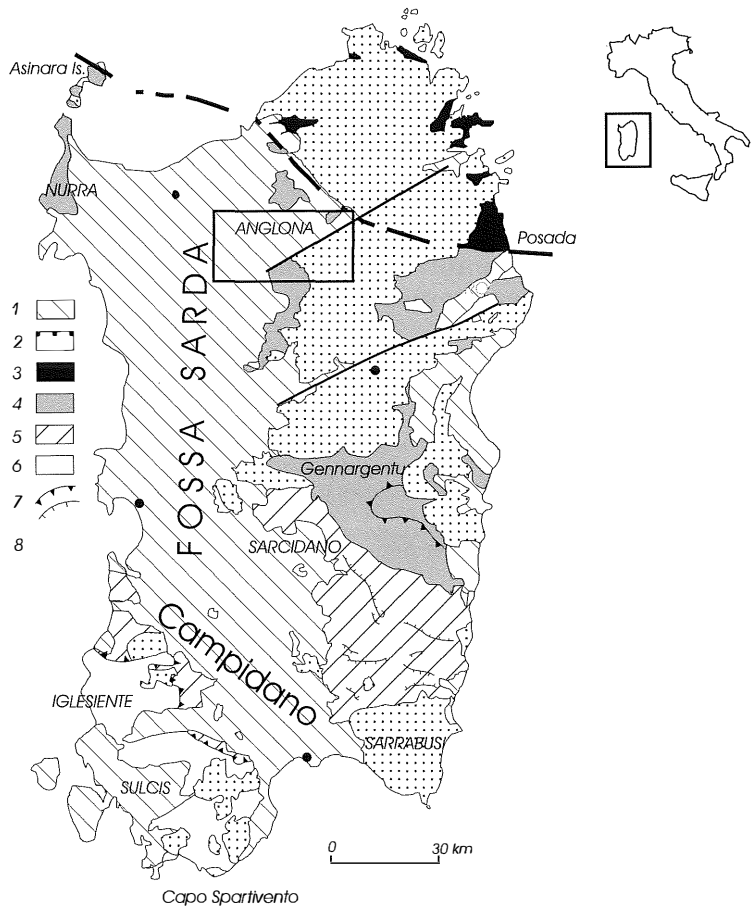

Fig. 1 – Study area (for more details, see Morbidelli *et al.*, 1999). Structural elements of Sardinian Basement are: 1) Post-Hercynian Cover, 2) Hercynian Batholith, 3) High Metamorphic Grade Complex, 4) Internal Nappe, 5) External Nappe, 6) External Zone, 7) Minor and Major Thrusts, 8) Posada-Asinara Line (after Carmignani, 1992, modified).

invece, viene confermato l'intervento di fluidi esterni.

KEY WORDS: *Clinoptilolite, Rietveld-RIR, chemistry, ignimbrites, base surges, epiclastic deposits.*

INTRODUCTION AND PETROGRAPHIC NOTES

It has recently become apparent that the Tertiary rhyodacitic ignimbrites of Sardinia (Italy) belonging to an orogenic calc-alkaline suite (Lecca *et al.*, 1997, and refs. therein) are extensively zeolitized (Ghiara *et al.*, 1995, 1997, 1999a, 1999b, 2000; Morbidelli, 1999; Morbidelli *et al.*, 1998, 1999). Zeolites are particularly abundant in whitish, poorly welded ash and pumice pyroclastic flows and related deposits (epiclastites and *base surges*). They often reach relative abundances, which are interesting as regards mining, and exploitation prospects have been described in recent papers (Langella *et al.*, 1998, 1999).

Clinoptilolite is the most widespread authigenic mineral, followed by smectite, opal and mordenite. Newly formed analcime and alkali feldspar also occurs locally.

In a recent paper on the regional distribution and textural features of authigenic minerals from pyroclastic flows outcropping in northern Sardinia (Morbidelli *et al.*, 1999), the following three genetic models were presented:

1. zeolite crystallising from entrapped cognate fluids in vugs and veins;
2. zeolite forming from alteration of glassy components (shards) from entrapped cognate fluids;
3. zeolite forming from alteration of glassy components from external fluids.

The latter minerogenetic model mainly applies to epiclastic and *base surge* deposits.

Cerri *et al.* (2001) recently proposed that hydrothermal fluids, mainly circulating through the fault system of the area, favoured zeolitization of Oligo-Miocene volcanoclastic rocks from Logudoro.

The present paper illustrates new data on the relative abundances and chemical compositions of the main authigenic phases. Research aims were to verify and better define the above minerogenetic models.

The sample area (fig. 1), about 350 km^2, lies near the villages of Bonorva, Ploaghe, Lula, Ozieri and Foresta Burgos. The area is part of a large structural depression known as «Fossa Sarda» and was infilled by ignimbrites and lacustrine sediments in the Lower Aquitanian-Burdigalian (Lecca *et al.*, 1997, and refs. therein).

The whitish, poorly welded ash and pumice pyroclastic flows may be mainly grouped into two formations, lower and upper (IC and ILP), respectively, emplaced mainly in a subaerial environment over a short period of time (Morbidelli *et al.*, 1999). The ILP ignimbrites are mostly flat, overlapping flow units, and frequently host degassing pipes; the IC ignimbrites are dominantly massive. All the pyroclastic flows are poorly sorted and display nearly similar petrographic features (Morbidelli *et al.*, 1999). Plagioclase (An_{68-30}), quartz, biotite, rare sanidine (Or_{80}) and Ca-rich pyroxene represent their phenocrystic association; amphibole is sporadic. Coarse, corroded quartz phenocrysts are not found in the IC ignimbrites.

Base surge (BS) and epiclastic (EV) deposits occur in the volcanic piles as discontinuous centimetric levels and/or greenish layers 5-10 m thick. Like the related pyroclastic deposits, the mineralogical assemblage is mainly represented by plagioclase grains, rounded quartz and biotite laths. The lithic component is made up of both welded and poorly welded ignimbrites, andesitic lavas and crystalline basement clasts. Major details on volcanic sequences, mineralogy and petrography of pyroclastites and epiclastites may be found in Morbidelli *et al.* (1999).

X-ray qualitative investigations are in good agreement with the mineralogical associations as identified under petrographic and scanning electron (SEM) microscopes (Morbidelli *et al.*, 1999; Ghiara *et al.*, 2000). On the whole, the mineralogical assemblages are as follows:

– primary magmatic minerals (phenocrysts to microphenocrysts) in both IC and ILP ignimbrites are: plagioclase, quartz, biotite, rare sanidine, Ti-magnetite, Ca-rich pyroxene and sporadic amphibole;

– main secondary minerals, in order of decreasing abundance, are: clinoptilolite, smectite, silica minerals (opal-CT, chalcedony, quartz), alkali feldspars and mordenite; calcite and glauconite mainly occur in the BS and EV deposits; analcime is occasional.

– considerable variations in secondary mineral contents, also occurring along vertical stratigraphic sections, are apparent from diffraction patterns.

Sampling and experimental methods

Representative rock samples, measuring up to 15 × 15 × 15 cm, of ILP and IC ignimbrites and related deposits (EV and BS) were ground

in a steel mortar, the complete crush was subdivided into four portions, and then one portion was powdered in a agate mortar to a final grain size less than 10 mm.

Qualitative phase analyses were performed using a PHILIPS PW 1830 diffractometer with unfiltered CuK_α radiation (40 KV, 20 mA). Data were recorded in the 3°-70° 2θ range, with a scanning speed of 1°/min and a time per step of 2 s/step, 1° divergence slit, 0.1 mm receiving slit, and 2° antiscatter slit.

Quantitative phase analysis data were collected on a SEIFERT PAD 4 diffractometer with a pyrolitic graphite analyzer crystal using unfiltered CuK_α radiation (40KV, 30 mA) in the 15°-120° 2θ range, with steps of 0.02° 2θ and a counting time of 18 s for each step, 0.5° divergence slit, 0.1 mm receiving slit, and 0.5° antiscatter slit.

Side loading was used for all samples to minimize preferred orientation effects.

A total of 26 representative samples, which were diluted with 10 and 30 wt% reference corundum standard material (NIST SRM 674a), were refined with the combined *Rietveld-RIR* (Reference Intensity Ratio) method (for details, see Chung, 1974a, 1974b; Artioli *et al.*, 1991; Snyder, 1992; Gualtieri and Artioli, 1995; Gualtieri 1996). Data were refined using the GSAS (*General Structure Analysis System*) computer package (Larson and Von Dreele, 1997).

Starting atomic coordinates for the phases were: clinoptilolite (Koyama and Takeuchi, 1977), quartz (Le Page and Donnay, 1976), plagioclase (Phillips *et al.*, 1971), K-feldspar (Ribbe, 1979), biotite (Ohta *et al.*, 1982), Ca-pyroxene (Makino and Tomita, 1989), smectite (Zheng and Bailey, 1989), mordenite (Meier, 1961), analcime (Cruciani and Gualtieri, 1999) and opal-CT (as cristobalite) (Dollase, 1965).

In GSAS, the background was successfully fitted with a Chebyshev function with 12 coefficients. Peak profiles were modelled using a pseudo-Voigt function with one Gaussian and one Lorenzian coefficient. Lattice constants, phase fraction, and coefficients corresponding to sample displacements and asymmetry were also refined. When satisfactory convergence of the calculated observed model was achieved, each crystalline and amorphous phase weight percent could be calculated by means of these equations:

$$W_{f,s} = W_{f,c} * W_s / W_{s,c}$$

for added 10 wt% reference α-Al_2O_3:

$$W_f = (100/90) * W_{f,s}$$

for added 30 wt% reference α-Al_2O_3:

$$W_f = (100/70) * W_{f,s}$$

where:

W_s= weight of internal standard;

W_f= f phase weight in mixture without internal standard;

$W_{f,s}$= f phase weight in mixture with internal standard;

$W_{f,c}$= f phase calculated weight in mixture with internal standard;

$W_{s,c}$= internal standard calculated weight;

$$W_a = 100 - \sum_{i=1}^{n} W_i$$

where W_a and W_i were the weight fractions of the i-th crystalline and amorphous phases, respectively. These data were used to draw a regression line.

To extrapolate data at zero contents of added internal standard, see details in Gualtieri (2000).

Chemical analyses were performed using a Cameca-Camebax microprobe with accelerating voltage of 15 KV for all elements, a sample current of 10 nA and a beam diameter of 10 μm. On-line corrections for drift, dead time and background were applied to raw data. Full corrections were made with the PAP program (Phouchu, 1984). Natural silicates (albite, periclase, corundum, wollastonite, orthoclase, hematite) were used as standard materials. Analytical precision was better than

TABLE 1

*Results of XRD quantitative analyses (wt%) for zeolite-bearing ignimbrites (IC and ILP), base surge (BS) and epiclastic (EV) deposits. Numbers in brackets: error quoted from GSAS (Larson and Von Dreele, 1997). R.T.= rock type. Clino= clinoptilolite, Qz = quartz, Pl = plagioclase, Bt = biotite, Smec = smectite, Px= pyroxene, Kf = K-feldspar, Mord = mordenite, Anal = analcime, Op= opal-CT, Am = amorphous components (glass+silica minerals), * = trace, - = not detected.*

Sample	Locality	R.T.	Clino	Qz	Pl	Bt	Smec	Px	Kf	Mord	Anal	Op	Am	Total
138.2B	M. Manias	IC	24 (±1)	23 (±3)	19 (±2)	3 (±1)	3 (±2)	1 (±1)	11 (±3)	-	-	2 (±2)	15 (±3)	101 (±2)
160.6	C. Majore	IC	42 (±2)	8 (±2)	17 (±2)	2 (±1)	2 (±2)	1 (±2)	12 (±2)	-	-	4 (±2)	11 (±3)	99 (±2)
160.9	C. Majore	IC	44 (±2)	7 (±2)	19 (±2)	1 (±1)	2 (±2)	1 (±1)	13 (±2)	-	-	5 (±2)	12 (±3)	104 (±2)
165.2	P.Ladu	IC	30 (±2)	19 (±2)	17 (±2)	3 (±1)	1 (±1)	1 (±1)	16 (±3)	-	-	-	13 (±3)	100 (±2)
184.1	S.A.Bisarcio	IC	6 (±1)	25 (±1)	17 (±2)	5 (±2)	5 (±2)	1 (±1)	19 (±1)	-	-	2 (±2)	22 (±4)	102 (±2)
190	M.S.Bernardo	IC	23 (±1)	22 (±1)	16 (±2)	4 (±1)	2 (±2)	1 (±1)	14 (±1)	-	-	1 (±1)	19 (±1)	102 (±1)
148	Sa Segada	IC	16 (±2)	18 (±2)	23 (±1)	4 (±l)	4 (±2)	2 (±2)	19 (±2)	-	-	-	15 (±1)	101 (±2)
70.2	C.D.Rosaria	IC	29 (±2)	23 (±2)	19 (±2)	3 (±1)	2 (±2)	1 (±1)	14 (±2)	-	-	-	12 (±2)	103 (±2)
120.1	M.Manias	ILP	21 (±1)	23 (±1)	19 (±1)	4 (±1)	2 (±2)	1 (±1)	15 (±2)	-	-	1 (±1)	15 (±2)	101 (±1)
179.1	P.Ladu	ILP	26 (±2)	19 (±2)	18 (±2)	3 (±1)	2 (±2)	1 (±1)	16 (±1)	-	-	1 (±1)	13 (±3)	99 (±2)
188.2.1	S.A.Bisarcio	ILP	6 (±1)	25 (±2)	17 (±2)	4 (±1)	3 (±2)	1 (±1)	16 (±3)	9 (±1)	*	1 (±1)	20 (±4)	102 (±2)
188.2.2	S.A.Bisarcio	ILP	3 (±1)	24 (±1)	17 (±1)	5 (±2)	4 (±2)	1 (±1)	16 (±2)	7 (±2)	*	3 (±2)	21 (±5)	101 (±2)
214.2	M. Fulcadu	ILP	13 (±1)	30 (±2)	20 (±2)	3 (±1)	1 (±1)	2 (±2)	16 (±2)	-	-	1 (±1)	15 (±2)	101 (±2)
205.3	M. Fulcadu	ILP	16 (±1)	29 (±3)	20 (±2)	3 (±1)	1 (±1)	2 (±2)	16 (±2)	-	-	-	14 (±3)	101 (±2)
147.1	Sa Segada	ILP	-	29 (±2)	22 (±2)	2 (±1)	-	1 (±1)	30 (±2)	-	-	-	17 (±2)	101 (±2)
MI 2.3	M. Inzos	ILP	30 (±2)	11 (±2)	22 (±2)	2 (±1)	3 (±2)	3 (±2)	10 (±2)	-	-	3 (±2)	17 (±3)	101 (±2)
BA 2.3	Badiamenta	ILP	35 (±2)	13 (±2)	19 (±2)	4 (±1)	3 (±2)	1 (±1)	10 (±3)	-	-	3 (±2)	17 (±2)	105 (±2)
GP 2.4	Giolzi Perra	ILP	34 (±2)	16 (±2)	19 (±2)	5 (±1)	3 (±2)	1 (±1)	7 (±2)	-	-	1 (±1)	18 (±2)	104 (±2)
CO 2.3	C.Oddorai	ILP	53 (±3)	9 (±2)	15 (±2)	2 (±1)	2 (±2)	1 (±1)	4 (±1)	-	-	5 (±2)	12 (±2)	103 (±2)
CP 2.3	C. Pinna	ILP	15 (±1)	19 (±2)	22 (±2)	3 (±2)	3 (±2)	2 (±2)	21 (±2)	-	-	-	16 (±4)	101 (±2)
101.1	M. Manias	BS	35 (±2)	12 (±1)	19 (±1)	4 (±1)	3 (±2)	1 (±1)	11 (±1)	-	-	1 (±1)	15 (±2)	101 (±1)
101.4	M: Manias	BS	53 (±2)	9 (±2)	12 (±2)	2 (±1)	2 (±2)	1 (±1)	7 (±2)	-	-	1 (±1)	13 (±2)	100 (±2)
130C	M.Manias	BS	45 (±2)	11 (±2)	15 (±3)	2 (±1)	3 (±2)	-	6 (±2)	-	-	7 (±2)	13 (±2)	102 (±2)
58aren	M.S.Bernardo	EV	21 (±1)	27 (±3)	17 (±2)	4 (±1)	1 (±1)	1 (±1)	13 (±1)	-	-	-	15 (±2)	99 (±1)
70	C.D.Rosaria	EV	17 (±1)	25 (±2)	21 (±2)	3 (±1)	2 (±2)	2 (±2)	14 (±2)	-	-	3 (±2)	14 (±2)	101 (±2)
RAS1.1	Abbialzu	EV	30 (±2)	14 (±3)	25 (±2)	3 (±2)	6 (±2)	1 (±1)	10 (±1)	-	-	-	13 (±3)	102 (±2)

TABLE 2

Final agreement factors for Rietveld-RIR factors. R.T. = rock type. N° Var= number of refined variables, N° Obs = number of observations.

Sample	Locality	R.T.	χ^2	R_{wp} (%)	N° Var.	N° Obs.
138.2B	M. Manias	IC	7.134	9.68	55	5250
160.6	C. Majore	IC	3.740	12.27	57	5250
160.9	C. Majore	IC	2.197	7.63	55	5250
165.2	P.Ladu	IC	3.821	14.10	60	5250
184.1	S.A.Bisarcio	IC	6.247	9.78	57	5247
190	M.S.Bernardo	IC	8.236	13.54	55	5250
70.2	C.D.Rosaria	IC	12.388	15,34	55	5250
148	Sa Segada	IC	9.437	13.78	57	5250
120.1	M..Manias	ILP	6.478	7.45	55	5249
179.1	P.Ladu	ILP	4.899	11.60	48	5247
188.2.1	S.A.Bisarcio	ILP	11.080	15.26	48	5249
188.2.2	S.A.Bisarcio	ILP	12.070	16.96	48	5250
214.2	M. Fulcadu	ILP	7.154	9.31	55	5249
205.3	M. Fulcadu	ILP	6.267	8.26	61	5247
147.1	Sa Segada	ILP	11.344	14.56	48	5270
MI 2.3	M. Inzos	ILP	5.488	11.80	52	5250
BA 2.3	Badiamenta	ILP	8.125	13.79	48	5247
GP 2.4	Giolzi Perra	ILP	9.126	14.16	48	5247
CO 2.3	C.Oddorai	ILP	4.934	12.27	48	5250
CP 2.3	C. Pinna	ILP	5.066	11.41	55	5250
101.1	M. Manias	BS	6.312	10.02	61	5249
101.4	M. Manias	BS	5.144	9.73	61	5250
130C	M. .Manias	BS	4.244	9.28	57	5250
58aren	M.S.Bernardo	EV	12.046	15.78	55	5250
70	C.D.Rosaria	EV	10.947	14.08	55	5250
RAS1.1	Abbialzu	EV	9.457	12.89	55	5220

3% for Si, Al, Fe, Mg, Ca and K, and better than 10% for Na.

RESULTS

X-ray quantitative investigations

The quantitative mineralogical analyses of 26 added samples belonging to ignimbrites (ILP and IC), *base surges* (BS) and epiclastic deposits (EV) are listed in Table 1.

Good agreement between calculated and observed patterns was observed, in accordance with the weighted agreement factor R_{wp} and χ^2 ($R_{wp}= S_y/\Sigma W_i(i_{io})^2$, where: S_y = residue, W_i = weight assigned to the i-th observation, I_{io} = measured intensity; $\chi^2 = S_y/N_o\text{-}N_v$ where S_y = residue, N_o = number of observed points, N_v =

number of refined points) of the refinements listed in Table 2.

The most important aspects for minerogenetic interpretation emerging from the overall quantitative data set listed in Table 1 are:

1. clinoptilolite contents vary widely in both IC and ILP ignimbrites, from 3 wt% to 53 wt%;

2. mordenite needles are widespread in the ignimbrites (i.e., Giolzi Perra and Sant'Antonio di Bisarcio sectors), but cannot often be detected by XRD owing to their small amounts;

3. analcime-bearing ignimbrites, occurring only near Sant'Antonio di Bisarcio, have low clinoptilolite contents;

4. smectite does not exceed 5 wt% in IC and ILP ignimbrites, and does not correlate with any other authigenic phase;

5. the alkali feldspar contents in several ignimbrites are higher than those inferred (2-6 wt%) by inspection of thin sections on phenocrystic to microphenocrystic components (Morbidelli *et al.*, 1999); some of them may therefore be assigned to newly formed phases, as clearly suggested by textural relationships with plagioclase grains or volcanic glass and chemical composition (see below);

6. significantly, some of the highly silicized rocks, showing fine-grained patches of anhedral and late silica-mineral aggregates, have higher alkali feldspar contents and lack zeolite (i.e., sample 147.1);

7. amorphous component contents (glass+opal) are poorly negative-correlated (R^2= 0.4514) with the amount of zeolite;

8. the measured alkali feldspar contents are poorly negative-correlated (R^2= 0.6861) with the amount of zeolite (fig. 2).

The zeolite contents of all the sampled rocks (80 ILP ignimbrites, 38 IC ignimbrites and 29 from BS and EV deposits) were calculated starting from refined diffraction patterns and using integrated areas of (020) for clinoptilolite and (200) for mordenite reflections. The results are shown in fig. 3.

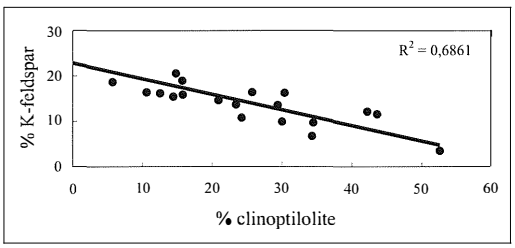

Fig. 2 – Clinoptilolite *vs* alkali feldspar contents (wt%).

About 55 samples of ILP ignimbrites fall in the class 10-27 wt% clinoptilolite, with peaks in the 19-27 wt% class; only 8 samples have high clinoptilolite (>40 wt%).

Among the latter samples, those from Case Oddorai (Bonorva area) are very important, since they show high average (36 wt%) clinoptilolite contents, up to 59 wt% in some levels of the cooling unit.

Fourteen samples from IC ignimbrites show peaks in the class 0-9 wt% clinoptilolite; the remaining 24 samples fall in the class 9-45 wt% clinoptilolite; only a few samples have high clinoptilolite (45 wt%).

The BS+EV deposits clearly show great variations in clinoptilolite contents. About half the samples fall in the class 0-27 wt% clinoptilolite and only 2 in the classes 37 and 54 wt%. It is interesting to note that clinoptilolite contents are lower in the fine-grained levels.

In order to identify horizontal to vertical small-scale mineralogical and petrographic variations, five stratigraphic sections from a small sector (Bonorva area) were sampled in detail (cfr. samples from Case Oddorai=CO, Monte Inzos=MI, Case Pinna=CP, Giolzi Perra=GP, Badiamenta=BA). Each section contains several flat, overlapping ILP ignimbritic flows, emplaced over a short period of time (Morbidelli *et al.*, 1999). All the discrete cooling units were sampled from bottom to top (i.e., CO 1.1-1.3 refer to the lower ignimbritic flow, CO 2.1-2.3 to the overlapping ignimbritic flow, and so on). The above stratigraphic sections, with respect to

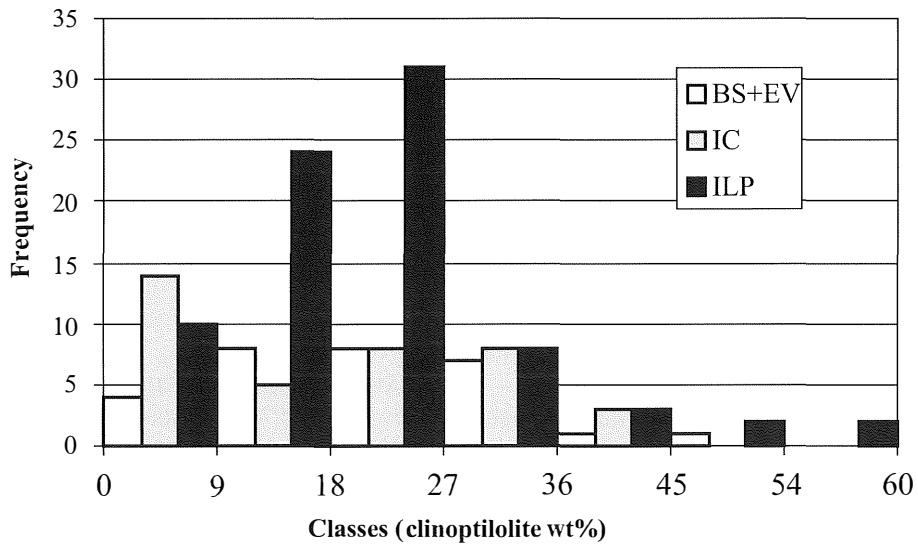

Fig. 3 - Histograms of clinoptilolite contents in zeolite-bearing ignimbrites and related deposits.

those reported in Ghiara *et al.* (2000), are not reconstructed and must therefore be considered real.

Vertical distributions of clinoptilolite amounts in the five stratigraphic sections from the Bonorva area are shown in fig. 4. Comparisons among the five sections reveal ample but not very obvious variations in clinoptilolite contents. In addition, careful comparisons among the single cooling units indicate that a general outline cannot be inferred for clinoptilolite zoning. It is interesting to note, however, that the upper portions of several cooling units are enriched in clinoptilolite.

Chemistry

The compositional trends of the main authigenic phases are illustrated in the following sections.

Clinoptilolite

The average analyses of individual crystals occurring in each sample of ILP ignimbrites are listed in Table 3. Clinoptilolite compositions of IC ignimbrites and BS and EV deposits are listed in Tables 4 and 5, respectively.

Clinoptilolites from ILP ignimbrites show ample compositional variations and, in the (Ca+Mg)-Na-K diagram (fig. 5), almost entirely overlap the field defined by Ghiara *et al.* (1997) for clinoptilolites in Sardinian Tertiary ignimbrites. As regards exchangeable cations, clinoptilolites continuously range from K- to Ca-clinoptilolite. However, as fig. 5 shows, most of them have alkalis in excess with respect to alkaline earth cations, with potassium as dominant cation.

With the exception of sample CO3.2, the Si/Al ratio of clinoptilolites varies between 4.31 and 5.25. A good negative correlation (R^2 = 0.90) is observed between divalent and monovalent cations, whose ratios continuously range from 0.46 to 2.06. Concerning alkali behaviour, only K contents are closely correlated with divalent cations.

With the exception of a few samples, clinoptilolites show narrow compositional

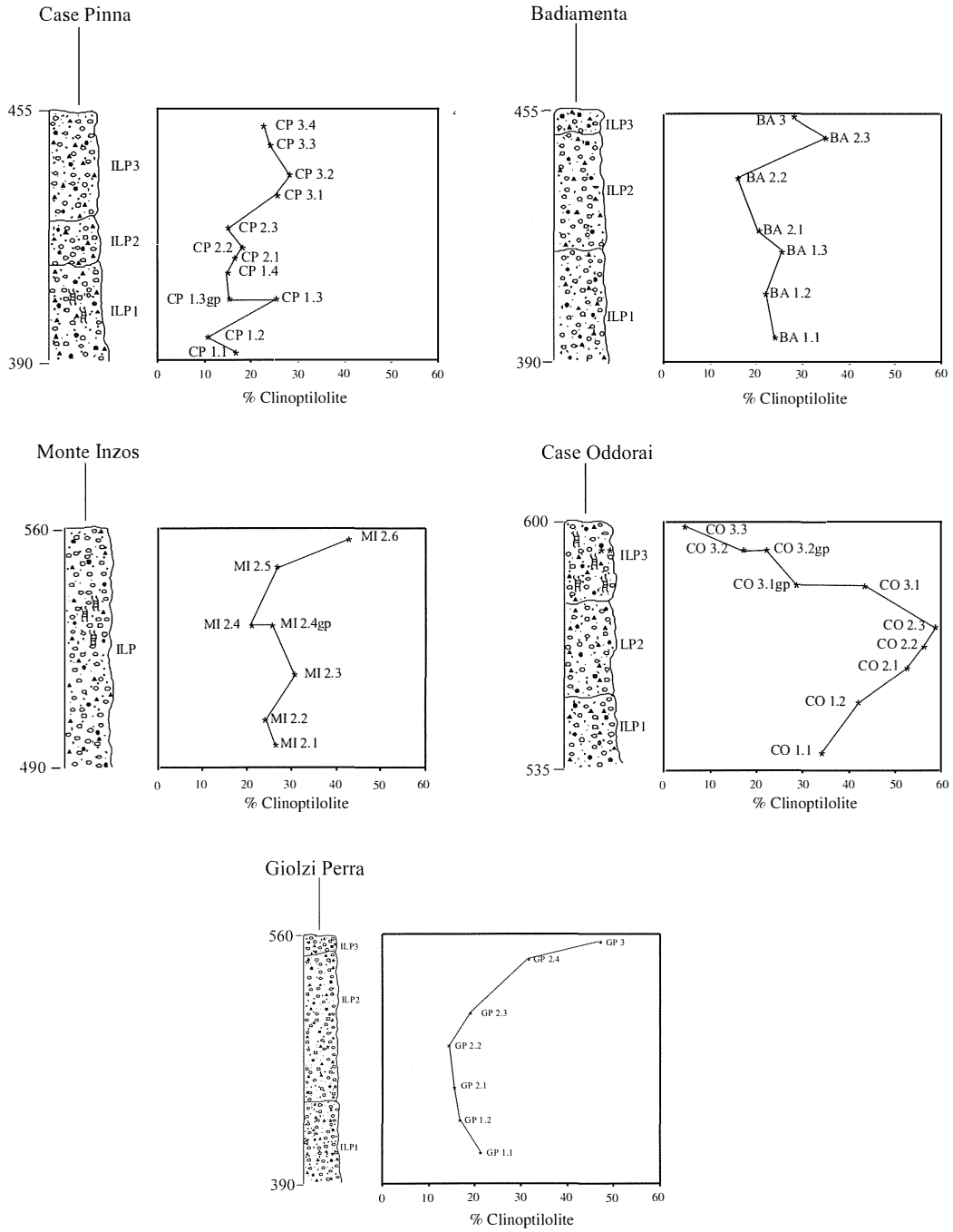

Fig. 4 - Stratigraphic sequences and clinoptilolite variations in wt% of ILP ignimbrites from Bonorva area. Elevations in metres. See text for major explanations.

TABLE 3

Representative microprobe analyses of clinoptilolites from ILP ignimbrites. All values given as weight % oxides; standard deviation in brackets; n.a= number of analysis points; S= clinoptilolite growing on cuspate glassy fragments; V= clinoptilolite lining vugs and tubular to subspherical vesicles; I= clinoptilolite intergrowing with silica minerals in patches; Gp= clinoptilolite in degassing pipes. Structural formulas based on 72 oxygens; —=not detected. E%= percent balance error: [(Al+Fe^{3+})-(Na+K)-2∗(Ca+Mg)]/(Al+Fe^{3+})∗100; D/M = divalent/monovalent cations.

Sample	AS 176 7764	AS 176 7764	AS184-2 7769	AS184-2 7769	AS 200 7777	AS 229A 7788	AS 229A 7788	AS 229B 7789	AS 70-2 7805	AS 160-6 7843	AS 160-9 7846	AS 160-9 7846	AS 141-1 7830	AS 179-1 7765
Locality	P. Ladu V	P. Ladu S	Bisarcio V	Bisarcio S	Bisarcio S	Sa Segada V	Sa Segada S	Sa Segada S	D. Rosaria S	C. Maiore V	C. Maiore V	C. Maiore S	M.Manias V	P. Ladu I
n.a.	3	3	4	4	1	5	2	1	3	6	2	2	5	5
SiO_2	67.42 (1.08)	67.51 (0.95)	65.35 (1.25)	65.71 (1.25)	66.64	70.26 (0.86)	71.41 (1.32)	68.65	66.34 (0.88)	67.38 (1.12)	65.66 (1.09)	63.32 (0.96)	66.73 (0.83)	67.54 (1.02)
Al_2O_3	12.37 (0.55)	12.17 (0.48)	11.83 (0.52)	11.90 (0.41)	12.36	11.86 (0.37)	12.02 (0.44)	11.10	11.91 (0.53)	12.10 (0.61	12.21(0.63)	11.58 (0.45)	11.92 (0.38)	11.44 (0.48)
Fe_2O_3	0.04 (0.02)	0.08 (0.03)	0.03 (0.01)	0.03 (0.02)	0.10	0.04 (0.03)	0.03 (0.01)	0.45	0.06 (0.02)	0.08 (0.02)	0.09 (0.03)	0.02 (0.01)	0.19 (0.04)	0.16 (0.08)
MgO	0.40 (0.09)	0.42 (0.05)	1.43 (0.11)	1.05 (0.08)	1.09	0.64 (0.02)	0.64 (0.02)	0.80	0.98 (0.05)	0.20 (0.05)	0.16 (0.02)	0.25 (0.06)	0.43 (0.01)	1.06 (0.08)
CaO	0.88 (0.12)	0.80 (0.18)	1.86 (0.22)	1.99 (0.15)	2.76	1.98 (0.09)	2.00 (0.21)	1.65	1.56 (0.11)	0.80 (0.09)	0.93 (0.21)	0.77 (0.16)	1.42 (0.14)	2.22 (0.15)
Na_2O	1.47 (0.18)	1.65 (0.10)	1.28 (0.09)	1.57 (0.11)	0.71	1.07 (0.15)	1.17 (0.09)	0.85	1.64 (0.11)	1.17 (0.15)	1.19 (0.18)	0.88 (0.10)	0.78 (0.01)	0.73 (0.08)
K_2O	6.43 (0.23)	5.93 (0.18)	1.68 (0.11)	1.70 (0.16)	2.00	3.43 (0.15)	3.49 (0.12)	3.75	2.51 (0.18)	7.81 (0.21)	7.16 (0.35)	8.03 (0.36)	6.17 (0.24)	2.54 (0.18)
Si	29.63	29.73	29.77	29.79	29.66	30.14	30.15	30.21	29.83	29.67	29.55	29.55	29.73	30.06
Al	6.41	6.32	6.35	6.36	6.48	6.00	5.98	5.76	6.31	6.28	6.48	6.36	6.26	6.00
Fe^{3+}	0.01	0.03	0.01	0.01	0.03	0.01	0.01	0.15	0.02	0.03	0.03	0.01	0.06	0.05
Mg	0.26	0.28	0.97	0.71	0.72	0.41	0.40	0.53	0.66	0.13	0.11	0.17	0.29	0.71
Ca	0.41	0.38	0.90	0.96	1.31	0.90	0.90	0.78	0.75	0.38	0.45	0.38	0.68	1.05
Na	1.25	1.41	1.13	1.38	0.62	0.89	0.96	0.73	1.43	1.00	1.04	0.80	0.67	0.63
K	3.61	3.33	0.98	0.98	1.14	1.88	1.88	2.11	1.44	4.39	4.11	4.77	3.51	1.44
E%	3.33	4.73	7.95	10.36	10.79	10.39	9.12	8.08	10.31	-1.49	3.85	-4.94	3.51	7.09
Si/Al	4.62	4.71	4.69	4.68	4.57	5.02	5.04	5.25	4.73	4.72	4.56	4.65	4.75	5.01
D/M	0.14	0.14	0.89	0.71	1.15	0.47	0.46	0.46	0.49	0.09	0.11	0.10	0.23	0.85

TABLE 3: *continued*

Sample	CO 1.1	CO 1.2	CO 2.1	CO 2.1	CO 2.2	CO 2.3	CO 3.1	CO 3.2	CO 3.3	CP 1.1	CP 1.2	CP 1.3	CP 1.4	CP 2.1
Locality	Oddorai S	Oddorai S	Oddorai S	Oddorai S	Oddorai S	Oddorai S	Oddorai Gp	Oddorai Gp	Oddorai S	C. Pinna S	C. Pinna S	C. Pinna G p	C. Pinna S	C. Pinna S
n.a.	6	8	4	1	7	3	1	1	1	4	6	6	7	1
SiO_2	66.52 (1.15)	67.87 (1.13)	69.07 (0.85)	69.87	67.88 (1.10)	68.17 (0.82)	67.50 (0.87)	68.63 (0.91)	67.00	69.24 (0.87)	69.31 (0.81)	69.20 (0.80)	68.42 (0.71)	70.57
Al_2O_3	12.53 (0.62)	12.29 (0.40)	12.60 (0.57)	13.04	11.87 (0.72)	12.15 (0.49)	12.34 (0.43)	10.32 (0.49)	12.00	12.65 (0.53)	12.76 (0.35)	12.61 (0.34)	12.69 (0.48)	12.68
Fe_2O_3	0.15 (0.04)	0.06 (0.02)	0.19 (0.05)	0.33	0.14 (0.01)	0.28 (0.01)	-	0.51 (0.01)	0.10	0.08 (0.03)	0.08 (0.02)	0.18 (0.01)	0.14 (0.01)	0.05
MgO	0.78 (0.03)	0.46 (0.02)	0.97 (0.04)	0.93	0.37 (0.04)	1.12 (0.01)	0.9 (0.01)	0.30(0.01)	0.40	0.86 (0.04)	0.78 (0.03)	0.84 (0.02)	1.14 (0.09)	1.50
CaO	2.50 (0.18)	1.72 (0.23)	2.97 (0.36)	2.25	1.05 (0.07)	1.93 (0.15)	3.0 (0.01)	0.82 (0.02)	1.60	1.88 (0.22)	2.10 (0.15)	2.09 (0.15)	2.54 (0.20)	2.44
Na_2O	0.76 (0.10)	1.54 (0.16)	0.46 (0.15)	1.02	0.90 (0.17)	0.51 (0.21)	0.4 (0.14)	0.64 (0.12)	1.70	1.21 (0.08)	0.66 (0.11)	0.82 (0.09)	0.59 (0.11)	0.68
K_2O	3.98 (0.16)	4.44 (0.15)	3.05 (0.17)	3.35	6.38 (0.29)	4.33 (0.26)	2.91 (0.13)	6.12 (0.15)	4.50	3.71 (0.13)	4.44 (0.18)	4.02 (0.19)	3.08 (0.14)	2.43
Si	29.48	29.73	29.65	29.53	29.87	29.72	29.74	30.51	29.77	29.71	29.67	29.70	29.61	29.83
Al	6.54	6.34	6.37	6.50	6.16	6.24	6.77	5.42	6.26	6.40	6.44	6.38	6.47	6.42
Fe^{3+}	0.05	0.02	0.06	0.11	0.05	0.09	-	-	0.02	0.03	0.03	0.06	0.05	0.02
Mg	0.51	0.30	0.62	0.59	0.24	0.73	0.56	0.22	0.29	0.55	0.50	0.54	0.79	0.94
Ca	1.18	0.80	1.36	1.02	0.49	0.90	1.40	0.39	0.75	0.86	0.96	0.96	1.29	1.10
Na	0.65	1.31	0.38	0.84	0.77	0.43	0.32	0.52	1.46	1.01	0.55	0.68	0.41	0.56
K	2.25	2.48	1.67	1.81	3.58	2.41	1.65	3.45	2.56	2.03	2.43	2.02	1.45	1.31
E%	4.62	5.96	5.93	9.93	5.44	3.92	7.63	7.14	7.04	8.83	8.88	8.74	7.75	4.35
Si/Al	4.51	4.69	4.65	4.54	4.85	4.76	4.39	5.63	4.76	4.64	4.61	4.66	4.58	4.65
D/M	0.58	0.29	0.97	0.61	0.17	0.57	0.99	0.15	0.26	0.46	0.49	0.56	1.12	1.09

TABLE 3: *continued*

Sample	CP 2.2	CP 2.3	CP 3.1	CP 3.1	CP 3.2	CP 3.2	CP 3.3	CP 3.3	CP 3.3	CP 3.4	CP 3.4	MI 2.1	MI 2.2
Locality	C. Pinna S	C. Pinna S	C. Pinna S	C. Pinna S	C. Pinna S	C. Pinna S	C. Pinna S	C. Pinna S	C. Pinna S	C. Pinna S	C. Pinna S	M. Inzos S	M. Inzos S
n.a.	3	8	4	3	3	3	4	2	2	5	3	6	7
SiO_2	68.52 (0.85)	67.99 (1.08)	68.33 (0.80)	68.50 (0.95)	68.97 (0.94)	69.89 (0.84)	69.23 (0.83)	69.84 (1.10)	69.12 (1.09)	67.81 (1.15)	68.18 (0.95)	69.70 (0.97)	69.63 (0.98)
Al_2O_3	12.59 (0.36)	12.84 (0.47)	12.75 (0.35)	12.69 (0.81)	12.70 (0.81)	12.81 (0.35)	12.58 (0.57)	12.70 (0.38)	12.72 (0.38)	12.58 (0.75)	12.84 (0.80)	12.76 (0.58)	12.74 (0.56)
Fe_2O_3	0.07 (0.01)	0.07 (0.01)	0.11 (0.02)	0.03 (0.02)	0.05 (0.01)	0.02 (0.01)	0.10 (0.06)	0.06 (0.02)	0.03 (0.01)	0.02 (0.01)	0.07 (0.01)	0.05 (0.03)	0.13 (0.04)
MgO	0.93 (0.01)	0.80 (0.02)	1.29 (0.11)	1.16 (0.02)	1.01 (0.08)	0.91 (0.03)	0.65 (0.05)	1.14 (0.01)	0.64 (0.03)	0.70 (0.02)	0.64 (0.03)	1.14 (0.02)	0.57 (0.06)
CaO	1.51 (0.21)	1.65 (0.16)	2.90 (0.28)	2.60 (0.17)	2.54 (0.01)	2.32 (0.11)	1.81 (0.25)	2.27 (0.23)	2.02 (0.20)	1.66 (0.10)	1.57 (0.11)	3.77 (0.05)	1.70 (0.18)
Na_2O	0.88 (0.11)	1.04 (0.06)	0.47 (0.10)	0.50 (0.16)	0.51 (0.16)	0.69 (0.20)	1.05 (0.09)	0.92 (0.07)	1.30 (0.07)	1.34 (0.05)	1.11 (0.10)	0.32 (0.06)	1.99 (0.09)
K_2O	4.49 (0.22)	5.16 (0.11)	2.14 (0.15)	2.83 (0.18)	3.14 (0.16)	3.59 (0.15)	4.63 (0.21)	2.98 (0.09)	3.79 (0.10)	4.79 (0.22)	5.53 (0.29)	1.50 (0.39)	3.63 (0.11)
Si	29.7	29.49	29.61	29.66	29.7	29.72	29.72	29.74	29.7	29.58	29.5	29.69	29.69
Al	6.43	6.56	6.51	6.48	6.44	6.42	6.37	6.37	6.44	6.47	6.55	6.41	6.40
Fe^{3+}	0.02	0.02	0.03	0.01	0.02	0.01	0.03	0.02	0.01	0.01	0.02	0.02	0.04
Mg	0.60	0.52	0.84	0.75	0.65	0.58	0.41	0.72	0.41	0.45	0.42	0.73	0.36
Ca	0.70	0.76	1.34	1.20	1.17	1.06	0.83	1.03	0.93	0.77	0.73	1.72	0.78
Na	0.74	0.88	0.39	0.42	0.42	0.57	0.87	0.76	1.08	1.14	0.93	0.27	1.65
K	2.48	2.85	1.18	1.56	1.73	1.95	2.54	1.62	2.08	2.66	3.05	0.82	1.98
E%	9.78	4.42	9.50	9.44	10.56	10.10	7.84	8.13	9.67	3.41	4.58	7.20	8.56
Si/Al	4.62	4.50	4.55	4.58	4.61	4.63	4.67	4.67	4.61	4.57	4.50	4.63	4.64
D/M	0.40	0.34	1.39	0.98	0.85	0.65	0.36	0.74	0.42	0.32	0.29	2.25	0.31

TABLE 3: *continued*

Sample	MI2.3	MI2.4	MI2.5	MI2.5	MI2.6	MI2.6	BA 1.1	BA 1.2	BA 1.2	Ba 1.3	BA 1.3	BA 2.1
Locality	M. Inzos S	M. Inzos Gp	M. Inzos S	M. Inzos S	M. Inzos S	M. Inzos S	Badiamenta S	Badiamenta S	Badiamenta S	Badiamenta S	Badiamenta S	Badiamenta S
n.a.	6	7	4	3	5	4	3	2	2	4	3	5
SiO_2	69.76 (0.98)	69.21 (0.87)	69.47 0.84)	70.01 (0.94)	69.16 (0.91)	69.50 (0.83)	70.29 (0.74)	69.97 (0.92)	70.24 (0.90)	69.03 (0.84)	68.87 (0.85)	69.46 (0.90)
Al_2O_3	12.69 (0.60)	12.75 (0.55)	12.72 (0.51)	12.76 (0.41)	12.81 (0.50)	12.75 (0.55)	12.40 (0.38)	12.45 (0.39)	12.30 (0.40)	12.50 (0.51)	12.50 (0.51)	12.62 (0.25)
Fe_2O_3	0.02 (0.01)	0.11 (0.03)	0.08 (0.03)	0.18 (0.01)	0.09 (0.02)	0.08 (0.03)	-	0.16 (0.01)	0.03 (0.02)	0.07 (0.01)	0.13 (0.02)	0.05 (0.03)
MgO	0.26 (0.03)	0.97 (0.05)	0.65 (0.02)	1.07 (0.09)	1.09 (0.07)	1.35 (0.02)	0.78 (0.02)	1.36 (0.01)	1.11 (0.02)	0.99 (0.04)	1.03 (0.01)	0.52 (0.01)
CaO	2.13 (0.16)	2.17 (0.09)	1.60 (0.12)	2.17 (0.19)	1.80 (0.16)	2.56 (0.19)	1.73 (0.19)	2.14 (0.19)	1.64 (0.22)	2.26 (0.34)	2.55 (0.15)	1.52 (0.10)
Na_2O	2.59 (0.11)	0.92 (0.17)	1.80 (0.15)	1.23 (0.09)	1.23 (0.07)	0.73 (0.08)	1.92 (0.09)	1.23 (0.07)	1.68 (0.05)	0.47 (0.10)	0.30 (0.25)	0.74 (0.18)
K_2O	3.01 (0.18)	3.68 (0.16)	4.03 (0.10)	2.85 (0.18)	4.15 (0.30)	2.76 (0.12)	3.06 (0.30)	1.92 (0.25)	2.56 (0.22)	4.23 (0.11)	3.33 (0.15)	6.16 (0.24)
Si	29.71	29.65	29.68	29.71	29.56	29.64	29.89	29.84	29.94	29.71	29.74	29.7
Al	6.37	6.44	6.41	6.38	6.45	6.41	6.21	6.26	6.18	6.34	6.36	6.36
Fe^{3+}	0.01	0.03	0.03	0.06	0.03	0.03	-	0.05	0.01	0.02	0.04	0.02
Mg	0.16	0.62	0.41	0.68	0.69	0.86	0.49	0.86	0.70	0.64	0.67	0.33
Ca	0.97	0.99	0.73	0.98	0.82	1.17	0.78	0.97	0.74	1.04	1.18	0.70
Na	2.14	0.77	1.49	1.01	1.02	0.60	1.58	1.02	1.38	0.39	0.25	0.62
K	1.63	2.01	2.20	1.55	2.26	1.50	1.66	1.04	1.39	2.32	1.83	3.36
E%	5.44	7.33	7.07	8.91	2.52	4.36	6.72	9.23	8.41	9.82	9.99	5.46
Si/Al	4.66	4.60	4.63	4.66	4.58	4.62	4.81	4.77	4.84	4.69	4.68	4.67
D/M	0.30	0.58	0.31	0.65	0.46	0.97	0.39	0.89	0.25	0.62	0.89	0.26

TABLE 3: *continued*

Sample	Ba 2.2	BA 2.3	BA 3	GP 1.1	GP 1.2	GP 2.1	GP 2.1	GP 2.2	GP 2.3	GP 2.4	GP 3
Locality	Badiamenta S	Badiamenta S	Badiamenta S	Giolzi Perra S	Giolzi Perra S	Giolzi Perra S	Giolzi Perra S	Giolzi Perra S	Giolzi Perra S	Giolzi Perra S	Giolzi Perra S
n.a.	5	10	5	7	10	5	4	7	10	6	4
SiO_2	69.33 (0.94)	67.90 (0.79)	69.08 (0.85)	70.01 (0.93)	67.81 (0.88)	68.99 (0.91)	69.13 (0.93)	71.36 (0.93)	69.61 (0.87)	69.30 (0.96)	69.78 (0.91)
Al_2O_3	13.03 (0.21)	13.37 (0.35)	12.55 (0.52)	13.35 (0.56)	12.62 (0.49)	12.85 (0.57)	12.69 (0.63)	12.57 (0.65)	13.31 (0.61)	12.73 (0.67)	12.73 (0.58)
Fe_2O_3	0.01 (0.03)	0.04 (0.02)	0.14 (0.01)	0.06 (0.01)	0.10 (0.01)	0.18 (0.02)	0.07 (0.01)	-	0.09 (0.03)	0.03 (0.06)	0.18 (0.01)
MgO	1.01 (0.03)	0.95 (0.03)	0.88 (0.02)	1.21 (0.01)	0.63(0.04)	0.84 (0.01)	0.85 (0.03)	0.60 (0.02)	0.54 (0.10)	0.63 (0.08)	0.99 (0.01)
CaO	1.62 (0.09)	2.19 (0.15)	1.74 (0.23)	2.37 (0.13)	1.73 (0.11)	2.98 (0.13)	2.91 (0.10)	1.60 (0.12)	1.44 (0.08)	2.75 (0.10)	1.04 (0.04)
Na_2O	1.75 (0.10)	0.52 (0.09)	0.95 (0.10)	1.18 (0.10)	0.77 (0.14)	1.24 (0.16)	0.67 (0.10)	2.30 (0.13)	1.19 (0.10)	1.52 (0.15)	2.26 (0.12)
K_2O	3.61 (0.16)	5.06 (0.36)	4.43 (0.26)	2.86 (015)	5.81 (0.16)	2.41 (0.17)	2.87 (0.15)	3.06 (0.09)	5.83 (0.14)	2.27 (0.11)	3.49 (0.14)
Si	29.54	29.28	29.7	29.47	29.52	29.55	29.69	29.92	29.47	29.69	29.67
Al	6.54	6.80	6.36	6.62	6.48	6.49	6.42	6.21	6.64	6.43	6.38
Fe^{3+}	-	0.01	0.04	0.02	0.03	0.06	0.02	-	0.03	0.01	0.06
Mg	0.64	0.61	0.59	0.76	0.41	0.54	0.54	0.38	0.34	0.40	0.63
Ca	0.74	1.01	0.77	1.06	0.80	1.36	1.33	0.72	0.65	1.25	0.47
Na	1.45	0.44	0.80	0.96	0.65	1.03	0.55	1.87	0.97	1.26	1.86
K	1.96	2.79	2.42	1.54	3.23	1.32	1.57	1.63	3.15	1.24	1.85
E%	4.52	5.18	7.06	7.69	2.03	6.06	8.13	4.81	8.49	8.70	7.72
Si/Al	4.52	4.31	4.67	4.45	4.56	4.55	4.62	4.82	4.44	4.62	4.65
D/M	0.40	0.50	0.42	0.73	0.31	0.81	0.88	0.31	0.24	0.66	0.30

TABLE 4

Representative microprobe analyses of clinoptilolites from IC ignimbrites. All values given as weight % oxides; standard deviation in brackets; n.a= number of analysis points. S= clinoptilolite growing on cuspate glassy fragments; V= clinoptilolite lining vugs and tubular to subspherical vesicles. Structural formulas based on 72 oxygens. E%= percent balance error: [(Al+Fe^{3+})-(Na+K)-2∗(Ca+Mg)]/(Al+Fe^{3+})∗100; D/M = divalent/monovolent cations.

Sample	AS 148 7756	AS 148 7756	AS 190 7771	AS 138-2B 7825	AS 165-2 7848
Locality	Sa Segada V	Sa Segada S	Bisarcio S	M. Manias V	P. Ladu V
n.a.	5	4	2	7	9
SiO_2	64.75 (1.09)	64.11 (1.52)	65.61 (0.95)	66.25 (1.15)	67.65 (1.14)
Al_2O_3	11.78 (0.32	11.44 (0.28)	11.61 (0.33)	12.22 (0.44)	12.49 (0.42)
Fe_2O_3	0.06 (0.02)	0.08 (0.03)	0.11 (0.02)	0.07 (0.02)	0.09 (0.03)
MgO	0.82 (0.12)	0.77 (0.09)	0.25 (0.09)	0.87 (0.15)	1.42 (0.09)
CaO	2.39 (0.22)	2.33 (0.31)	3.52 (0.52)	2.26 (0.11)	2.94 (0.21)
Na_2O	0.75 (0.10)	0.81 (0.12)	1.51 (0.09)	1.29 (0.15)	1.01 (0.18)
K_2O	3.26 (0.21)	3.12 (0.11)	0.88 (0.09)	2.41 (0.06)	1.24 (0.10)
Si	29.7	29.79	29.89	29.69	29.61
Al	6.37	6.27	6.24	6.45	6.44
Fe^{3+}	0.02	0.03	0.04	0.02	0.03
Mg	0.56	0.53	0.17	0.58	0.93
Ca	1.17	1.16	1.71	1.08	1.37
Na	0.67	0.73	1.33	1.12	0.86
K	1.91	1.85	0.51	1.38	0.69
E%	5.55	5.37	10.62	10.13	5.03
Si/Al	4.66	4.75	4.79	4.60	4.60
D/M	0.67	0.66	1.02	0.66	1.48

variations within each sample. In addition, no significant compositional variations occur between clinoptilolites growing on cuspate shards and those lining tubular to subspherical vesicles hosted in pumiceous fragments (i.e., samples 7769 and 7846). Instead, very large compositional variations occur within both the volcanic piles and each ignimbritic flow. These variations do not follow obvious trends in all investigated stratigraphic sections. In particular, from the lower to intermediate-upper portions of each ignimbritic flow (i.e., GP 2-1 to GP 2-3), clear Na and K increases are observed in the volcanic sequences of Giolzi Perra (fig. 6*a*). Only in the upper part of each ignimbritic flow does a weak decrease in alkali contents occurs (GP2-4). In the volcanic

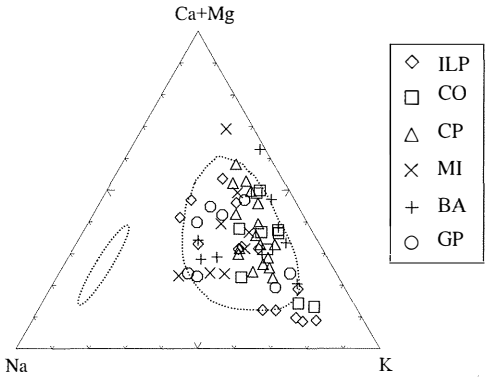

Fig. 5 - (Ca+Mg)-Na-K atomic % plot of clinoptilolites from ILP ignimbrites. Compositional range of clinoptilolites in Sardinian Tertiary ignimbrites after Ghiara *et al.* (1997), dotted lines. See text for explanations.

TABLE 5

Representative microprobe analyses of clinoptilolites from BS and EV deposits. All values given as weight % oxides; standard deviation in brackets; n.a= number of analysis points. Pm= clinoptilolite patches growing on crystal-vitric matrix; V= clinoptilolite hosted in veins. Structural formulas based on 72 oxygens. E%= percent balance error: [(Al+Fe^{3+})-(Na+K)-2(Ca+Mg)]/(Al+Fe^{3+})*100; D/M = divalent/monovalent cations.*

Sample	AS 70 7719	AS 151 7757	AS 151 7757	AS 58A 7803	AS 58A 7803	AS 138-3 7829	AS 241-1 7870	AS 175-5 7763	AS 101-1 7814	AS 101-4 7817
Locality	D. Rosaria Pm	D. Rosaria Pm	D. Rosaria V	Bernardo Pm	Bernardo Pm	M. Manias V	P. Udduri V	P. Ladu V	M. Manias Pm	M. Manias Pm
n.a.	3	5	2	3	5	1	5	3	10	5
SiO_2	68.28 (1.26)	66.76 (1.32)	68.87 (1.01)	67.62 (0.98)	67.64 (1.15)	68.94	66.72 (1.11)	63.79 (0.98)	66.44 (0.85)	68.20 (1.10)
Al_2O_3	12.43 (0.45)	12.25 (0.52)	12.76 (0.51)	12.04 (0.48)	12.46 (0.37)	12.77	12.21 (0.35)	12.21 (0.51)	12.13 (0.38)	12.34 (0.51)
Fe_2O_3	0.13 (0.08)	0.09 (0.02)	0.20 (0.08)	0.46 (0.11)	0.28 (0.12)	0.12	0.14 (0.02)	0.14 (0.10)	0.04 (0.02)	0.02 (0.01)
MgO	1.09 (0.11)	0.50 (0.08)	0.89 (0.12)	0.97 (0.06)	0.99 (0.03)	0.86	0.95 (0.11)	0.95 (0.12)	0.36 (0.02)	0.36 (0.12)
CaO	2.64 (0.21)	3.18 (0.19)	3.48 (0.22)	3.54 (0.15)	3.24 (0.09)	2.15	1.66 (0.25)	1.66 (0.21)	2.55 (0.16)	2.55 (0.10)
Na_2O	1.58 (0.18)	0.93 (0.10)	0.49 (0.06)	0.62 (0.05)	0.92 (0.09)	1.25	1.28 (0.11)	1.28 (0.08)	2.66 (0.18)	2.48 (0.22)
K_2O	0.98 (0.16)	2.36 (0.20)	1.85 (0.17)	0.93 (0.11)	1.42 (0.12)	3.09	3.19 (0.15)	3.19 (0.09)	1.11 (0.09)	1.25 (0.11)
Si	29.73	29.70	29.65	29.78	29.63	29.66	29.63	29.48	29.73	29.76
Al	6.41	6.42	6.48	6.25	6.43	6.48	6.52	6.65	6.40	6.35
Fe^{3+}	0.04	0.03	0.07	0.15	0.09	0.04	0.04	0.05	0.01	0.02
Mg	0.71	0.33	0.57	0.64	0.65	0.55	0.76	0.65	0.24	0.50
Ca	1.23	1.51	1.60	1.66	1.51	0.99	1.57	0.82	1.22	1.05
Na	1.33	0.80	0.41	0.53	0.78	1.04	0.48	1.15	2.31	2.10
K	0.54	1.34	1.02	0.52	0.79	1.70	0.71	1.88	0.70	0.70
E%	10.96	9.77	11.86	11.73	10.73	10.73	10.81	10.86	8.5	7.38
Si/Al	4.64	4.77	4.77	4.77	4.58	4.58	4.55	4.43	4.65	4.69
D/M	1.04	0.86	1.52	2.19	1.96	0.56	1.96	0.49	0.49	0.55

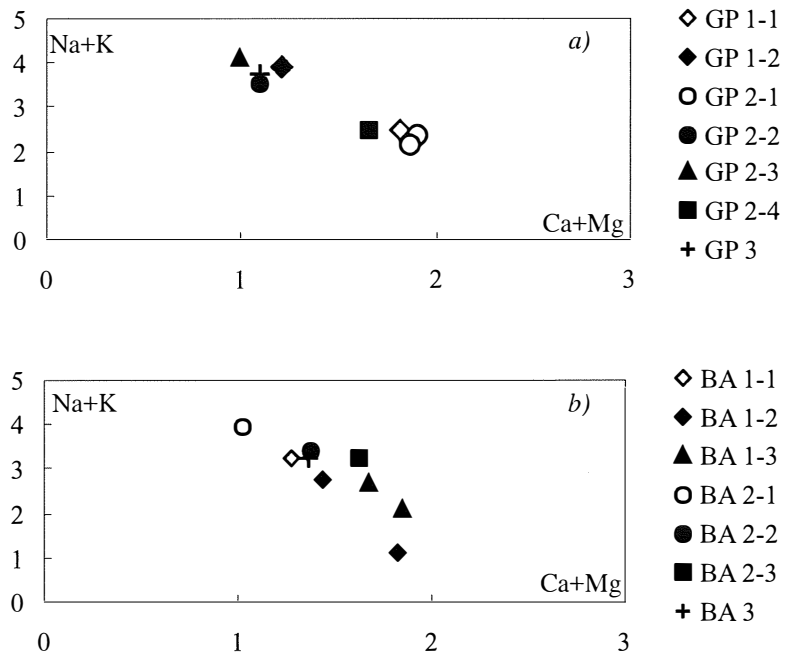

Fig. 6 - Compositional variations (Ca+Mg *vs* Na+K) of clinoptilolites in ILP volcanic sequences from Giolzi Perra (*a*) and Badiamenta (*b*). For further explanations on sample stratigraphic distributions, see also text and fig. 5.

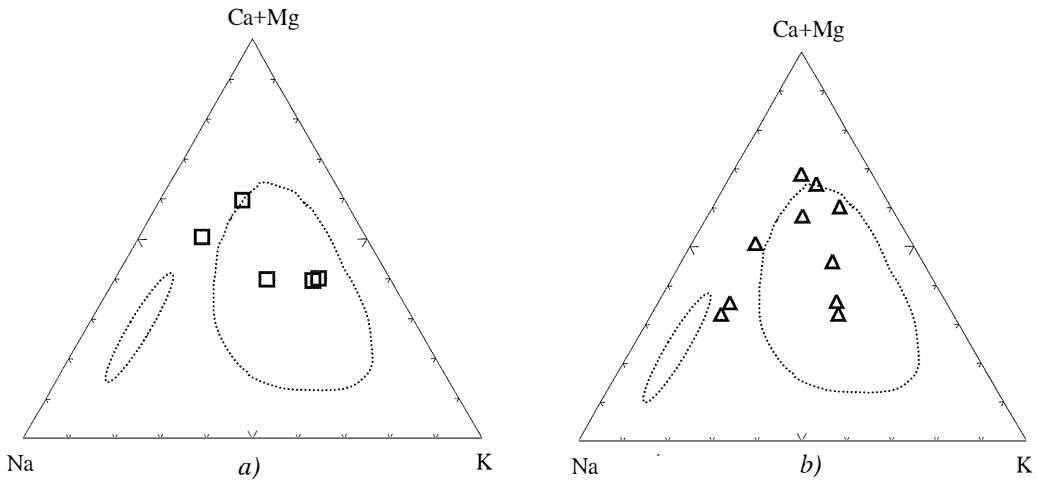

Fig. 7 - Compositional variations (Ca+Mg-Na-K) of clinoptilolites in IC ignimbrites *a*) and in *base surge* and epiclastic deposits *b*). Compositional range of clinoptilolites in Sardinian Tertiary ignimbrites after Ghiara *et al.* (1997), dotted lines. See text for explanations.

TABLE 6

Representative microprobe analyses of mordenites from IC and ILP ignimbrites. Samples 1-6 from Ghiara et al. (1997). All values given as weight % oxides. Structural formulas based on 96 oxygens. E%= percent balance error: [(Al+Fe^{3+})-(Na+K)-2(Ca+Mg)]/(al+Fe^{3+})*100.*

Sample	1 7590	2 7581	3 7562	4 6327	5 5614	6 6331	AS 188.2.1 7852	AS 188.2.2 7853
Locality	Bonorva ILP	Bonorva ILP	Bonorva ILP	Ozieri ILP	Bonorva ILP	Ozieri ILP	Bisarcio ILP	Bisarcio ILP
SiO_2	71.06	71.87	71.64	68.33	72.23	69.84	69.17	68.91
Al_2O_3	11.95	11.68	11.11	12.36	11.71	11.88	11.33	11.62
Fe_2O_3	0.17	0.04	0.22	0.10	0.48	0.01	0.06	0.05
MgO	1.11	0.23	0.27	0.19	0.11	0.03	0.17	0.14
CaO	2.94	3.81	3.82	3.41	3.14	2.46	3.10	2.84
Na_2O	0.76	0.97	0.90	1.94	2.61	1.98	2.00	2.56
K_2O	1.27	1.27	0.95	1.44	0.66	2.58	0.77	1.20
Si	40.16	40.43	40.67	39.67	40.27	40.08	40.38	40.12
Al	7.96	7.75	7.43	8.46	7.70	8.04	7.80	7.97
Fe^{3+}	0.07	0.02	0.09	0.04	0.20	0.00	0.03	0.02
Mg	0.94	0.19	0.23	0.16	0.09	0.03	0.15	0.12
Ca	1.77	2.28	2.31	2.11	1.87	1.51	1.93	1.76
Na	0.83	1.06	0.99	2.19	2.82	2.20	2.26	2.89
K	0.92	0.91	0.68	1.07	0.47	1.89	0.57	0.89
E%	9.50	9.86	10.19	8.22	8.71	11.57	10.58	5.55
Si/Al	5.05	5.22	5.47	4.69	5.23	4.99	5.18	5.03

sequences of Case Oddorai and M. Inzos, clinoptilolite compositional variations (not shown) are comparable with those of Giolzi Perra. Opposite trends are observed for volcanic sequences from Badiamenta (fig. 6*b*), in which weak increases in Ca and Mg contents occur in the upper part of each ignimbritic flow. Lastly, in the volcanic sequences of Casale Pinna (not shown), the uppermost ignimbritic flows display typical Giolzi Perra trends, whereas the opposite behaviour (Badiamenta trend) is observed in the lower ones.

The compositional variations of clinoptilolites from IC ignimbrites are similar to those of the ILP illustrated above. Their Si/Al and (Na+K)/(Ca+Mg) ratios range from 4.60 to 4.75 and 0.66 to 1.48, respectively. In the (Ca+Mg)-Na-K diagram (fig. 7*a*), the clinoptilolites of IC ignimbrites plot in the intermediate to upper portions, lacking typically alkali-rich varieties.

The clinoptilolites in the BS and EV deposits display Si/Al and (Na+K)/(Ca+Mg) ratios ranging from 4.43 to 4.77 and 0.49 to 2.19, respectively (fig. 7*b*). No significant compositional variations occur between clinoptilolites growing in patches on crystal-vitric matrixes and those hosted inside late veins. The BS and EV clinoptilolites differ from most of those occurring in the ILP and IC ignimbritic deposits due to the following compositional characteristics:

1) several specimens have high bivalent cation contents (up to 2.30 a.f.u);

2) some specimens have very high Na contents (up to 2.31 a.f.u);

3) a negative correlation between Ca+Mg and Na is observed for clinoptilolites growing on crystal-vitric matrixes.

TABLE 7

Representative microprobe analyses of authigenic K-feldspar and Na-rich plagioclase from IC and ILP ignimbrites. All values given as weight % oxides. Structural formulas based on 32 oxygens. Molecular end-member in mol%.

Sample	AS 100C 7810	AS 241.1 7870	AS 70.2 7805	AS 214.2 7864	AS 200 7777	CO 2.2
Locality	M. Manias IC	Bernardo ILP	D. Rosaria IC	M. Fulcadu ILP	S.A.Bisarcio ILP	C. Oddorai ILP
SiO_2	62.22	65.87	67.30	66.26	66.96	68.12
Al_2O_3	16.44	17.80	17.62	17.91	20.32	19.23
Fe_2O_3	0.42	0.11	0.09	0.11	0.02	—
CaO	0.38	0.02	0.01	0.02	1.31	0.4
Na_2O	0.94	0.27	0.25	0.28	10.32	11.21
K_2O	12.78	15.20	15.28	15.2	0.82	0.80
Si	12.17	12.16	12.25	12.16	11.79	11.97
Al	3.79	3.87	3.78	3.88	4.22	3.98
Fe^{3+}	0.06	0.02	0.01	0.02	—	—
Ca	0.08	—	—	—	0.25	0.08
Na	0.36	0.11	0.09	0.11	3.52	3.82
K	3.19	3.58	3.55	3.56	0.18	0.18
Or	87.9	97.0	97.5	97.0	4.7	4.4
Ab	9.9	3.0	2.5	3.0	89.1	93.8
An	2.2	0.0	0.0	0.0	6.2	1.8

It should be noted that K-rich clinoptilolite varieties are lacking in the BS and EV deposits.

Mordenite

Representative microprobe analyses of mordenites are given in Table 6. The extra-framework cation contents vary, with Na/(Na+Ca) in the range 0.30-0.62. Note that several mordenites plot outside the typical range (0.5-0.81) reported in Coombs *et al.* (1998).

Alkali feldspar

Convincing evidence that some feldspars, both sodic and potassic, are authigenic phases is offered by the following textural relationships:

a) adularia-like feldspar grows on the external rinds of altered shards or on plagioclase phenocrysts with epitaxial relationships;

b) clinoptilolites and alkali feldspars intergrow in fine-grained patches and/or within sub-spherical vesicles.

It is important to emphasize that the formation of zeolite from alkali feldspar precursors was not observed (see below).

Representative microprobe analyses of authigenic alkali feldspars from ignimbrites are listed in Table 7. As expected, when compared with phenocrystic feldspars, authigenic ones are nearly ideal in composition. K-feldspar and Na-rich plagioclase range in composition from Or_{88-98} and Ab_{89-94}, respectively. Most K-feldspars have no or very low Ca contents.

DISCUSSION

The whole data set of the chemistry of clinoptilolite and its quantitative distribution in the ignimbritic formations, together with textural features (Morbidelli *et al.*, 1999),

indicate that minerogenetic models should consider the following aspects:

1) there are considerable variations in both chemical compositions and amounts of clinoptilolites;

2) the above variations are observed inside both a single ignimbritic flow and a cooling unit;

3) textural and distribution relationships between the main newly-formed phases (clinoptilolite, mordenite, smectite, silica minerals, alkali feldspar) are clearly defined and indicate the early appearance of smectite and clinoptilolite (Morbidelli *et al.*, 1999; Ghiara *et al.*, 2000).

It is common knowledge that the above-mentioned aspects primarily depend on several factors, including: *a)* the mineralogical and petrographic composition of precursors; *b)* the chemical compositions of interacting fluids and rock/interacting fluid ratios; *c)* pH (Hay and Sheppard, 1977; Hall, 1988); *d)* temperature and pressure; *e)* type of operating system (closed or open); *f)* thermodynamic mineral stability; and *g)* late superimposed changes.

Concerning the investigated rocks and their alteration environments, it is important to recall that all the ignimbrites are very similar from the petrographic and volcanological viewpoints and that they underwent similar post-depositional events (Morbidelli *et al.*, 1999).

As regards interacting fluids, the textural and distribution features of the authigenic phases strongly suggest the dominant role played by cognate fluidising components of the ignimbrites in alteration processes (Morbidelli *et al.*, 1999). Some particular locally observed assemblage and textural relationships also require sudden changes in interacting fluid compositions and/or supply of external fluids (Ghiara *et al.*, 2000).

From the whole data set of the degree of zeolitization of poorly welded ignimbrites and related deposits, it emerges that:

1) large variations in authigenic mineral contents occur in both ignimbrites and BS and EV deposits;

2) no significant relationship exists between clinoptilolite contents and sample position in the examined stratigraphic sequences.

Our quantitative data, when compared with the results obtained by Ghiara *et al.* (1997) and Langella *et al.* (1999), on samples from the same volcanic area, reveal slightly lower opal-CT and clinoptilolite amounts. At present, on the basis of the quantitative data set available, it is difficult to define an average value of clinoptilolite contents in poorly welded ignimbrites, mainly because samples showing deep zeolitization have been repeatedly sampled and studied for mining reasons. Nevertheless, it is our opinion that, on a regional scale, clinoptilolite contents ranging from 20 to 30 wt% may be considered realistic for most of the poorly welded ignimbrites. On this basis, fluid amounts necessary to produce the above zeolite abundances are compatible with those already known in undegassed rhyolitic magmas in subvolcanic environments (Hamilton *et al.*, 1964; Johnson *et al.*, 1994; Barclay *et al.*, 1996), and the addition of extraneous fluids is not an essential requirement. It is also appropriate to take into account here the interbedded *base surge* deposits, which are typically hydromagmatic products. The deeply zeolitized levels may be explained by minerogenetic models based on late fluid concentrations within some portions of the ignimbritic flow and/or cooling unit.

In summary, the different degrees of zeolitization (points 1 and 2) are probably related to variations in the solid/interacting fluid ratios and/or the cooling rate of the ignimbritic flow. This strongly supports a minerogenetic model dominated by circulating cognate fluids, which were entrapped and concentrated or escaped from the deposits along gas pipes, as previously hypothesized on textural and distributive bases by Morbidelli *et al.* (1999).

As regards zeolite from *base surge* (BS) and epiclastic (EV) deposits, the mineral association of authigenic phases (cf. smectite, glauconite, zeolite, calcite), the chemical composition of clinoptilolite (cf. abundance of Ca-varieties) and extra-framework trends (Na

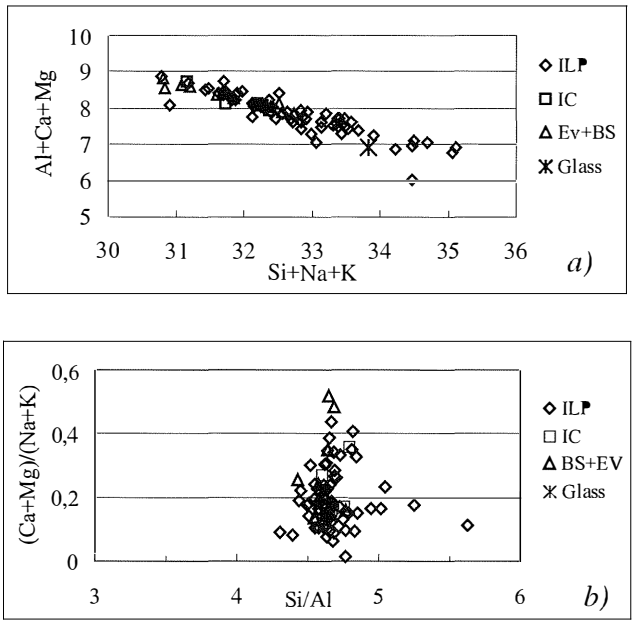

Fig. 8 – *a)* (Si+Na+K) *vs* (Al+Ca+Mg) and *b)* (Si/Al) *vs* (divalent/monovalent cations) diagrams of clinoptilolites in ignimbrites and related deposits. Unaltered glass composition also plotted.

negatively correlated with divalent cations) suggest another minerogenetic model. The low clinoptilolite contents in the fine-grained levels with respect to the coarse-grained ones clearly suggest reduced circulation of interacting fluids, probably due to a lower degree of porosity. In addition, textural features indicate that zeolitization in the EV deposit is mainly not syn-sedimentary (cf. clinoptilolite growing on the matrix in patches and lining veins). All these considerations fit the proposed minerogenetic model (Morbidelli *et. al.*, 1999) which requires external fluids related to groundwater circulation.

The overall data set of clinoptilolite chemistry defines a trend compatible with theoretical substitution pairs such as [Si+Na+K]- [Al+Ca+Mg] (fig. 8*a*).

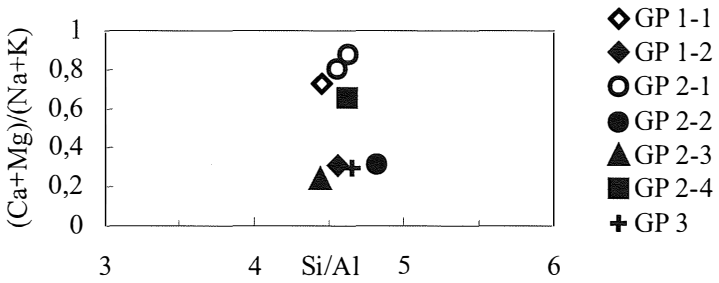

Fig. 9 – (Si/Al) *vs* (divalent/monovalent cations) diagram of clinoptilolites in ILP ignimbrites from Giolzi Perra sequence.

Substitutions involving framework cations are more obvious in the (Ca+Mg)/(Na+K) *vs* Si/Al diagram (fig. 8*b*) in which, except for a few samples, the clinoptilolites clearly show quite small changes in Si/Al ratios, clustering around 4.67. As a consequence, the main substitutions regard extra-framework cations with exchanges such as [Na+K]-[Ca+Mg].

In addition, close inspection of fig. 8 reveals that clinoptilolites from the IC ignimbrites and related deposits (BS and EV) have a smaller compositional range when compared with those of the ILP ignimbrites, lacking in the former strongly alkaline varieties.

It is interesting to note that changes in the divalent/monovalent ratio also occur on a small scale, as documented by clinoptilolites sampled along the stratigraphic sequence of a cooling unit (fig. 9).

Therefore, it is very probable that the different divalent/monovalent ratios represent a primary and distinctive character, rather than the results of compositional changes due to overlapping processes.

Since the starting materials within a ignimbritic flow may be considered closely comparable, minerogenetic models explaining sharp compositional variations and/or zonal arrangements of authigenic clinoptilolites require changes in some factors, i.e., composition of interstitial fluids and temperature. In addition, referring to the above-mentioned clinoptilolite distribution in the examined ignimbrites, several peculiar micro-systems may be hypothesised within the single ignimbritic flows during alteration processes.

Concerning changes in the chemical compositions of interacting fluids, it is important to recall that the dissolution process of a rhyodacitic glass, followed by crystallisation of secondary phases (i.e., smectite and clinoptilolite), produces residual liquids enriched in silica and alkalis. This is well documented by the geochemical balances of alteration processes carried out by Ghiara *et al.* (1999a, 1999b, 2000) and by the unaltered glass plots in the Al+Ca+Mg *vs* Si+Na+K diagram (fig. 8a). These fluids may migrate through the deposits, interact with glassy components and/or mix with other resident fluids. In summary, in the present case it is reasonable to hypothesise interacting fluids with slight chemical differences. Fluid migration towards the upper portion of the cooling unit during fumarole activity may easily explain several distinctive aspects of zeolite-bearing ignimbrites requiring changes in interacting fluid chemical composition. One important aspect is the zonal arrangement of clinoptilolites and/or sharp changes in their chemical composition. It is important to recall that comparable zonal arrangements of clinoptilolite varieties have been observed in several investigated stratigraphic sequences.

Field evidence of circulating mineralised fluids are widespread in the investigated ignimbrites (Morbidelli *et al.*, 1999; Ghiara *et al.*, 2000). Among these, the reddish, silicized facies, often observed in the upper parts of a cooling unit, have been interpreted as portions of ignimbrites diffusely permeated by silica-rich fluids. Lastly, vugs, patches and/or veins showing intergrowths of silica minerals and zeolites are textural evidence for circulating mineralised fluids and also indicate that the above-mentioned zeolites formed as primary chemical precipitates. The best evidence of circulating fluids is given by mineralogical and petrographic examination of degassing pipes, in which veins of felt-form clinoptilolite aggregates cementing phenoclastic and lithoclastic components occur (Photo 1). For these aggregates, textural relationships suggest crystallisation from circulating fluids, not glass alteration. In addition, newly formed silica-mineral patches (quartz, opal-CT, chalcedony) are well represented within the pipes (Photo 2).

All the above considerations fit the low correlation between amorphous components (glass and opal) and clinoptilolite amounts, suggesting that shard alteration is not the only minerogenetic process at work, since some zeolites may be due to precipitation from circulating fluids.

Another important factor capable of causing

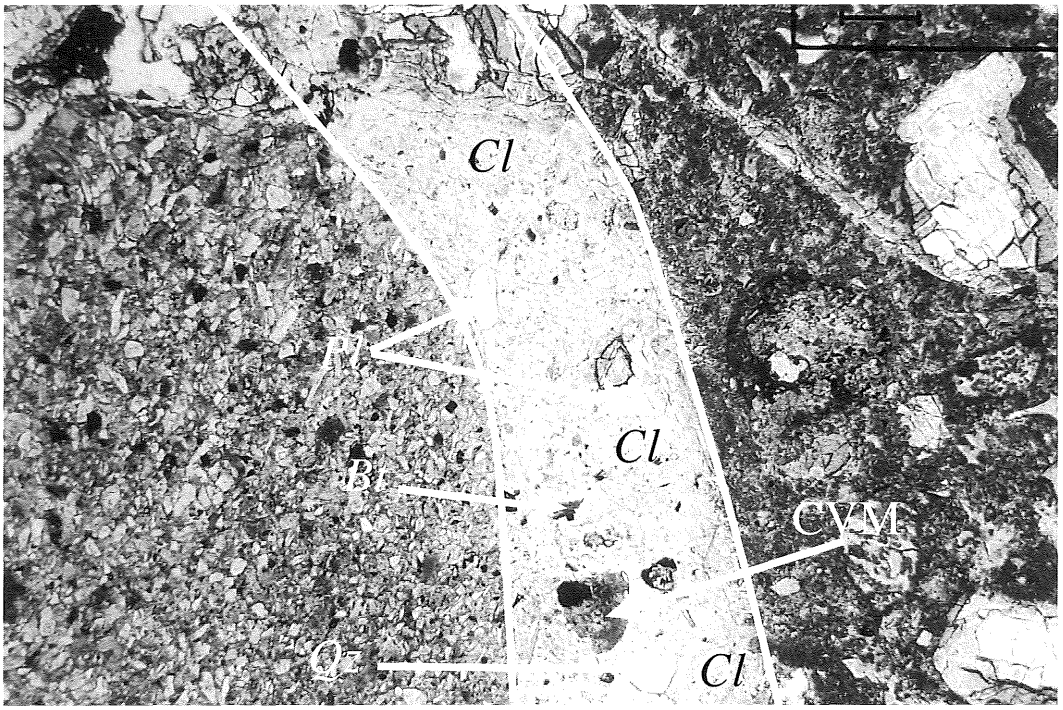

Photo 1 – Plane polarised, scale bar = 1 mm. Degassing pipes from Casale Fresu (Bonorva area). Vein of felt-form clinoptilolite aggregates (Cl) cementing plagioclase (Pl), biotite (Bt), quartz (Qz) and crystal vitric matrix (CVM).

significant differences in the chemical compositions and distribution features of authigenic phases is temperature, well documented in several worldwide occurrences.

Zeolite distribution in areas of hydrothermal alteration often exhibits well-defined zoning (Hay, 1975, and refs. therein). Clinoptilolite and mordenite often occur in the shallowest and coolest zones, whereas heulandite, analcime and wairakite prevail deeper. Zeolites formed by burial diagenesis in a thick column of silicic volcanic sediments display vertical zoning arrangements. In the upper zones, alteration of silicic glass produces montmorillonite, alkali clinoptilolite, alkali mordenite and opal-CT; in the deeper zones, previously formed early zeolites are transformed into analcime and then into albite. It is interesting to note that, in this reaction series, alkali clinoptilolite first changes into Ca-rich clinoptilolite. According to Iijima (1977), the above reaction series occurring in silica-saturated environments are mainly controlled by temperature. In summary, temperature increases promote the stability of Ca-rich varieties of clinoptilolite-heulandite series, and/or analcime and, lastly, alkali feldspar as stable phases.

In the whole study area, clear-cut information on these aspects of zeolite zoning arrangements, newly formed K-feldspar, and/or other distributions of stable phases is missing. In addition, it must be recalled that evidence for higher-temperature alteration processes have only been identified in a small sector (Sa Segada), where the ILP ignimbrites are strongly silicized and newly formed adularia grows on the external rinds of shard fragments (sample 147.1; Table 1). Significantly, zeolites are lacking in these ILP ignimbrites.

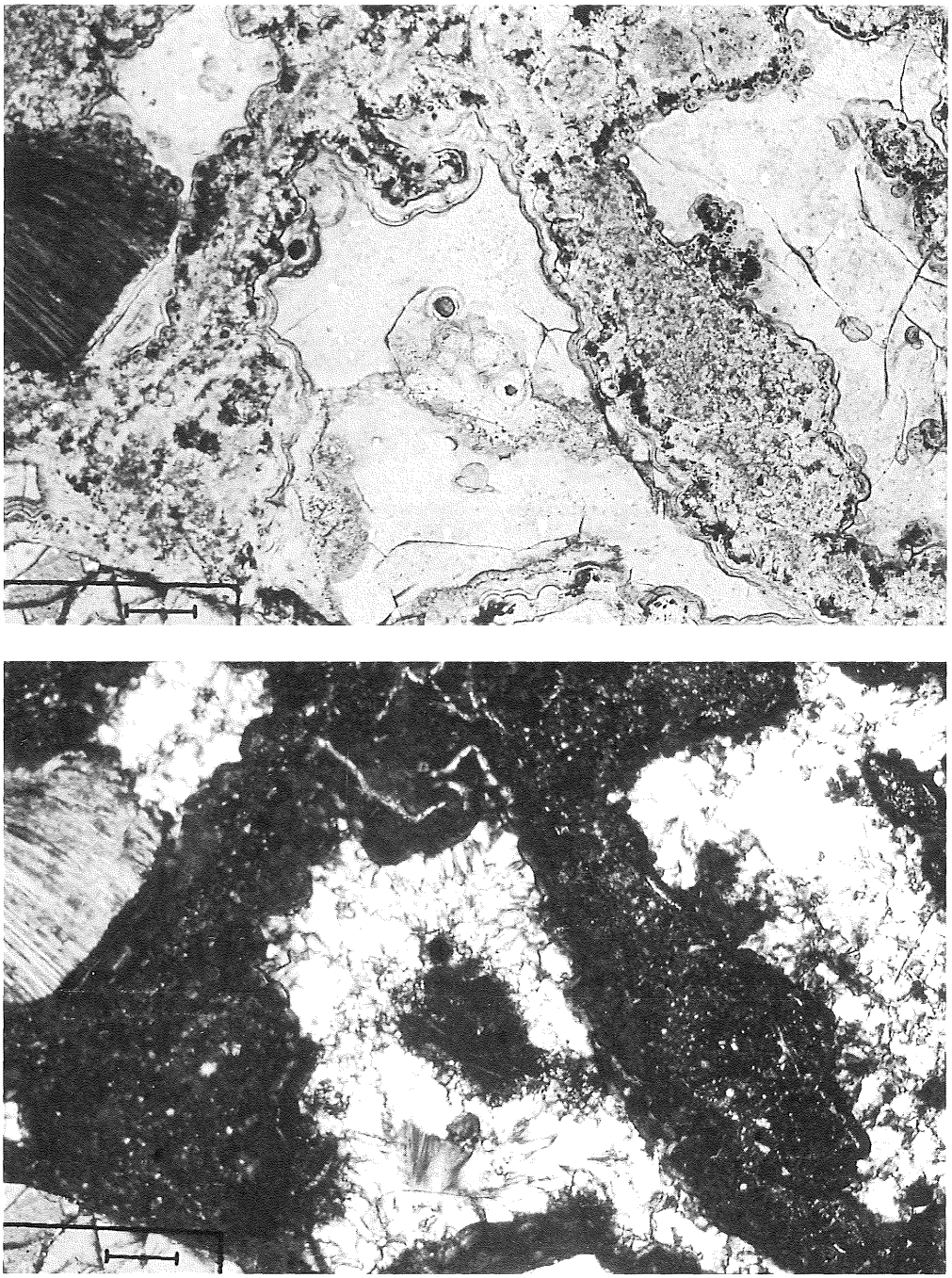

Photo 2 – Silica mineral patches in degassing pipes from Casale Fresu (Bonorva area); seale bar = 1 mm. *a)* Plane polarised and *b)* cross-polarised.

Concerning the examined stratigraphic sections, Ca-rich varieties of clinoptilolite are often found at the base of single cooling units, followed by alkali clinoptilolites in the upper portions (i.e., Giolzi Perra, Case Oddorai and Monte Inzos sections), whereas the opposite occurs in other sections (i.e., Badiamenta). Therefore, referring to the influence of temperature on the chemical composition of clinoptilolite, no obvious trends may be inferred from their distribution inside the ignimbritic cooling units. On this basis, our opinion is that temperature and/or thermal gradients represent a minor factor in the distribution of zeolite varieties in zeolite-bearing ignimbrites. As a consequence, the major factor seems to be the chemical composition of interacting fluids.

CONCLUSIONS

The quantitative distribution and chemical composition of clinoptilolites in ignimbrites from northern Sardinia show ample variations on both small and regional scales. These variations cannot be attributed to particular differences in starting products or volcanological and post-depositional geological histories.

The small-scale variations strongly suggest the presence of several, peculiar micro-systems within ignimbritic flows and/or cooling units during alteration processes.

The large range of clinoptilolite composition, from K to Ca, requires chemical changes in interacting fluids, which may also be produced during alteration processes. Indeed, the geochemical balance clearly indicates that glass dissolution, followed by smectite and zeolite crystallisation, produces residual liquids enriched in silica and alkalis.

Chemical differences in interacting fluids fit the mineralogical scenario of authigenic phases, revealing great variations in chemical composition. In ignimbritic rocks, authigenic phases show the following textural distribution:

1) filling vugs;

2) growing on glassy components;

3) intergrowing in patches randomly distributed in the matrix.

Minerogenetic models capable of causing great differences in both the alteration degree and chemical composition of zeolites are those connected with interacting fluids of cognate origin, which may be entrapped, chemically modified, and locally concentrated or helped to escape from deposits during later fumarole activity.

In summary, the quantitative distribution and chemical composition of the authigenic phases strongly support the three genetic models proposed on textural bases and illustrated in the introduction to the present paper.

ACKNOWLEDGMENTS

The authors are grateful to Prof. P. Brotzu for helpful suggestions and discussions to improve the paper. The present version benefited from comments and revisions by Profs. A. Gualtieri and B. Bigioggero. The authors also thank R. Carampin (Centro di Studio per la Geodinamica Alpina, CNR Padova) for his help in performing microprobe analyses.

This research was carried out with grants from Italian CNR n° 98.006177.CT11.

REFERENCES

ARTIOLI G., ALBERTI G., CAGOSSI G. and BELLOTTO M. (1991) — *Quantitative determination of crystalline and amorphous components in clinoptilolite-rich rocks by Rietveld analyses of X-ray powder diffraction profiles.* Atti I Convegno Nazionale di Scienza e Tecnologia delle Zeoliti, Colella C. ed., De Frede, Napoli, 261-270.

BARCLAY J. CARROLL M.R., HOUGHTON B.F. and WILSON C.J.N. (1996) — *Pre-eruptive volatile content and degassing history of an evolving peralkaline volcano.* J. Volcanol. Geotherm. Res., **74**, 75-87.

CARMIGNANI L. (1992) — *A tentative geodinamic model for the Hercinian basament of Sardinia.* I.G.C.P. n. 276, Newsletters, Siena, **5**, 61-82.

CERRI G., CAPPELLETTI P., LANGELLA A. and DE' GENNARO M. (2001) — *Zeolitization of Oligo-Miocene volcanoclastic rocks from Logudoro (northern Sardinia, Italy).* Contrib. Mineral. Petrol., **140**, 404-421.

CHUNG F.H. (1974a) — *Quantitative interpretation of X-ray diffraction patterns of mixtures. I. Matrix-flushing method for quantitative multicomponent analyses.* J. Appl. Cryst., **7**, 519.

CHUNG F.H. (1974b) — *Quantitative interpretation of X-ray diffraction patterns of mixtures. II. Adiabatic principle of X-ray diffraction analyses of mixtures.* J. Appl. Cryst., **7**, 526.

CRUCIANI G. and GUALTIERI A. (1999) — *Dehydration dynamics of analcime by in situ synchroton powder diffraction.* Am. Mineral., **84**, 112-119.

COOMBS D.S., ALBERTI A., ARMBRUSTER T. , ARTIOLI G., COLELLA C., GALLI E., GRICE J.D., LIEBAU F., MANDARINI J., MINATO H., NICKEL E., PASSAGLIA E., PEACOR D., QUARTIERI S., RINALDI R., ROSS M., SHEPPARD R., TILLMANNS E. and VEZZALINI G. (1998) — *Recommended nomenclature for zeolite minerals: report of the Subcommittee on Zeolites of the International Mineralogical Association, Commission on New Minerals and Mineral Names.* Eur. J. Mineral., **10**, 1037-1081.

DOLLASE W.A. (1965) — *Reinvestigation of the structure of low cristobalite.* Z. Kristallogr., **121**, 369-377.

GHIARA M.R., LONIS R., PETTI C., FRANCO E., LUXORO S. and BALASSONE G. (1997) — *The zeolitization process of Tertiary orogenic ignimbrites from Sardinia: distribution and mining importance.* Per. Mineral., **66**, 211-231.

GHIARA M.R., PETTI C., FRANCO E. and LONIS R. (1999b) — *Distribution and genesis of zeolites in Tertiary ignimbrites from Sardinia: evidence of superimposed mineralogic processes.* In: «Natural Zeolites for the Third Millennium» C.Colella and F.A. Mumpton (Eds.), 177-192.

GHIARA M.R., PETTI C., FRANCO E. and LONIS R. (2000) — *Distribution and genesis of zeolites in Tertiary ignimbrites from Sardinia: evidence of superimposed mineralogenic processes.* In: «Natural Zeolites for the Third Millennium», C. Colella and F.A. Mumpton (Eds.) 177-192.

GHIARA M.R., PETTI C., FRANCO E., LONIS R. and LUXORO S. and GNAZZO L. (1999a) — *Occurrence of clinoptilolite and mordenite in Tertiary calc-alcaline pyroclastites from Sardinia (Italy).* Clays and Clay Minerals, **47**, 319-328.

GHIARA M.R., PETTI C., FRANCO E., LUXORO S. and GNAZZO L. (1995) — *Diagenetic clinoptilolite from pyroclastic flows of northern Sardinia.* Proc. «3° Convegno Nazionale Scienza e Tecnologia delle Zeoliti» R. Aiello (Ed.), De Rose, Montalto (CS), 349-353.

GUALTIERI A. (1996) — *Modal analyses of pyroclastic rocks by combined Rietveld and RIR method.* Pow. Diff., **11**, 1-10.

GUALTIERI A. (2000) — *Accuracy of XRPD QPA using the combined Rietveld-RIR method.* J. Appl. Cryst., **33**, 267-278.

GUALTIERI A. and ARTIOLI G. (1995) — *Quantitative determination of chrysotile asbestos in bulk materials by combined Rietveld and RIR methods.* Pow. Diff., **11**, 1-10.

HALL A. (1998) — *Zeolitization of volcanoclastic sediments: the role of temperature and pH.* J. Sediment. Res, **68**, 5, 739-745.

HAMILTON W., BURNHAM C.V. and OSBORN E.F. (1964) — *The solubility of water and effects of oxygen fugacity and water content on crystallization in mafic magmas.* J. Petrol., **5**, 21-39.

HAY R.L. (1975) — *Geologic occurrence of zeolites.* In: «Natural Zeolites», L.B. Sand and F.A. Mumpton (Eds.) 135-143.

HAY R.L. and SHEPPARD R.A. (1977) — *Zeolites in open hydrologic systems.* In: Mumpton F.A. (Ed.) «Mineralogy and Geology of natural zeolites», Mineral. Soc. Am. Rev. Mineral., **4**, 93-102.

IIJIMA A. (1997) — *Geological occurrences of zeolites in marine environments.* In: «Natural Zeolites», L.B. Sand and F.A. Mumpton (Eds.) 175-198.

JOHNSON M.C., ANDERSON A.T. JR and RUTHERFORD M.J. (1994) — *Pre-eruptive volatile contents of magmas.* Mineral. Soc. Am. Rev. Mineral, **30**, 67-121.

KOYAMA K. and TAKEUCHI Y. (1977) — *Clinoptilolite: the distribution of potassium atoms and its role in thermal stability.* Z. Kristall., **145**, 216-239.

LANGELLA A., CAPPELLETTI P., CERRI G., BISH D.L. and DE' GENNARO M. (1999) — *Distribution of industrial minerals in Sardinia: Clinoptilolite bearing rocks of the Logudoro region.* In: «Natural Microporous Materials in Environmental Technology», P. Misaelides *et al.* (Eds.), 237-252.

LANGELLA A., CAPPELLETTI P., CERRI G and DE GENNARO M. (1998) — *Prospection of industrial minerals in Sardinia: zeolites of heulandite group in Logudoro volcaniclastites.* Proc. «4° Convegno Nazionale Scienza e Tecnologia delle Zeoliti» E. Fois and A. Gamba (Eds.), Centro di Cultura Scientifica A. Volta, Como, Italy, 128-131.

LARSON A.C. and VON DREELE R.B. (1997) — *GSAS. General Structure Analysis System.* - Report LAUR 86-748, Los Alamos National Laboratory, Los Alamos, New Mexico.

LECCA L., LONIS R., LUXORO S., MELIS F., SECCHI F. and BROTZU P. (1997) — *Oligo-Miocene volcanic sequences and rifting stages in Sardinia: a review.* Per. Mineral., **66**, 7-61.

LE PAGE Y. and DONNAY G. (1976) — *Refinement of*

the crystal structure of low quartz. Acta Cryst., B32, 2456.

MAKINO K. and TOMITA K. (1989) — *Cation distribution in the octahedral sites of hornblendes.* Am. Mineral., **74**, 1097-1105.

MEIER W.M. (1961) — *The crystal structure of mordenite (ptilolite).* Z. Kristall., **115**, 439-450.

MORBIDELLI P. (1999) — *Distribuzione, caratterizzazione e genesi delle clinoptiloliti e dei minerali associati nelle piroclastiti Terziarie della Sardegna settentrionale.* Ph.D. thesis, Università «La Sapienza», Rome, Italy.

MORBIDELLI P., GHIARA M.R., LONIS R. and FRANCO E. (1998) — *Clinoptilolite distribution in Tertiary ignimbrites from Bonorva (Central Sardinia, Italy).* Proc. «4° Convegno Nazionale Scienza e Tecnologia delle Zeoliti», E. Fois and A. Gamba (Eds.), Centro di Cultura Scientifica A. Volta, Como, Italy, 166-171.

MORBIDELLI P., GHIARA M.R., LONIS R. and SAU A. (1999) — *Zeolitic occurrences from pyroclastic flows and related epiclastic deposits outcropping in northern Sardinia (Italy).* Per. Mineral., **68**, 287-313.

OHTA T., TAKEDA H., TAKEUCHI Y. (1982) — *Mica polytypism; similarities in the crystal structures of coexisting 1M and 2M (sub 1) oxybiotite.* Am. Mineral., **67**, 298-310.

PHILLIPS M., COLVILLE A.A., RIBBE P.H. (1971) — *The crystal structures of two oligoclases; a comparison with low and high albite.* Z. Kristall., **133**, 43-65.

PHOUCHU J.L. (1984) — *A new model for X-ray microanalysis.* La Recherche Aérospatial, **3**, 167-192.

RIBBE P.H. (1979) — *The structure of a strained intermediate microcline in cryptoperthitic association with twinned plagioclase.* Am. Mineral., **64**, 402-408.

SNYDER R.L. (1992) — *The use of Reference Intensity Ratios in X-ray quantitative analysis.* In: «Powder Diffraction», May-December.

ZHENG H. and BAILEY S.W. (1989) — *Structures of intergrown triclinic and monoclinic IIb chlorites from Kenya.* Clays and Clay Minerals, **37**, 308-316.